Molecular Biology of the Cell
Vol. 12, 3550–3562, November 2001

Cytoskeleton-dependent Membrane Domain Segregation during Neutrophil Polarization

Stéphanie Seveau,* Robert J. Eddy, Frederick R. Maxfield,† and Lynda M. Pierini†

Department of Biochemistry, Weill Medical College of Cornell University, New York, New York 10021

Submitted April 5, 2001; Revised July 10, 2001; Accepted August 16, 2001
Monitoring Editor: W. James Nelson

On treatment with chemoattractant, the neutrophil plasma membrane becomes organized into detergent-resistant membrane domains (DRMs), the distribution of which is intimately correlated with cell polarization. Plasma membrane at the front of polarized cells is susceptible to extraction by cold Triton X-100, whereas membrane at the rear is resistant to extraction. After cold Triton X-100 extraction, DRM components, including the transmembrane proteins CD44 and CD43, the GPI-linked CD16, and the lipid analog, $DiIC_{16}$, are retained within uropods and cell bodies. Furthermore, CD44 and CD43 interact concomitantly with DRMs and with the F-actin cytoskeleton, suggesting a mechanism for the formation and stabilization of DRMs. By tracking the distribution of DRMs during polarization, we demonstrate that DRMs progress from a uniform distribution in unstimulated cells to small, discrete patches immediately after activation. Within 1 min, DRMs form a large cap comprising the cell body and uropod. This process is dependent on myosin in that an inhibitor of myosin light chain kinase can arrest DRM reorganization and cell polarization. Colabeling DRMs and F-actin revealed a correlation between DRM distribution and F-actin remodeling, suggesting that plasma membrane organization may orient signaling events that control cytoskeletal rearrangements and, consequently, cell polarity.

INTRODUCTION

A prerequisite for directed migration is the acquisition of a polarized morphology. Cellular polarization and motility require that separate regions of the cell adopt different properties to carry out specialized functions. At the front of the cell, the plasma membrane extends forward and adheres to the substratum, whereas in a coordinated manner, the back of the cell contracts and detaches from the substratum (Bretscher, 1996; Lauffenburger and Horwitz, 1996; Mitchison and Cramer, 1996). A central question in the understanding of cell migration is how these asymmetries are spatially organized and maintained. We hypothesized that plasma membrane compartmentalization into different domains could provide an important component of the spatial orientation leading to development and maintenance of cell polarity.

Studies on membrane composition provide evidence that lipids and proteins can be organized into microdomains in the plasma membrane (Brown and Rose, 1992; Brown and London, 1998a). Some types of microdomains are often called rafts because they are thought to exist as discrete zones within the plasma membrane where some lipids and proteins segregate on the basis of their phase separation behavior (Brown and Rose, 1992; Simons and Ikonen, 1997; Brown and London, 1998b). These microdomains have been characterized as cholesterol- and glycolipid-enriched membrane fractions that can be isolated on the basis of their resistance to extraction by cold nonionic detergents (called detergent-resistant membrane domains [DRMs]) and flotation to the low-density fraction of sucrose density gradients. Microdomains have been proposed to exclude selectively some molecules, or recruit and activate others, thereby forming signaling and sorting centers (Brown and Rose, 1992; Field *et al.*, 1997; Simons and Ikonen, 1997; Deans *et al.*, 1998; Keller and Simons, 1998; Rietveld and Simons, 1998).

A role for cholesterol-dependent lipid domains in cell migration has been proposed on the basis of the observation that disruption of domain integrity by depletion of plasma membrane cholesterol inhibited polarization and migration (Manes *et al.*, 1999; our unpublished data), whereas other cellular functions such as adherence were unaffected. One possibility is that specialized membrane domains function to segregate signaling molecules to the appropriate ends of

† Corresponding authors. E-mail addresses: frmaxie@med.cornell.edu or lpierini@med.cornell.edu.
*Present address: Département de Bactériologie et de Mycologie, Unité des Interactions Bactéries-Cellules. Institut Pasteur, France; e-mail: sseveau@pasteur.fr.

polarized cells. To accomplish this, membrane domains with different properties must be asymmetrically distributed in polarized cells. In support of this possibility, a panel of membrane proteins (CD44, CD43, ICAM-1, and PSGL-1), some of which have been shown to be in DRMs in other cell types, are asymmetrically distributed at the surface of migrating cells (Jacobson *et al.*, 1984; Sanchez-Madrid and del Pozo, 1999; Seveau *et al.*, 1997, 2000). In the case of these transmembrane proteins, it is unclear whether their distribution is controlled by the distribution of DRMs or by other factors such as an association with the cytoskeleton. Also, cytoskeleton-associated transmembrane proteins may control the distribution of DRMs, because aggregation of the transmembrane receptor FcεRI has been shown to cause a co-redistribution of DRMs (Thomas *et al.*, 1994; Holowka *et al.*, 2000).

CD44, the major hyaluronate receptor, is a type I transmembrane glycoprotein that is abundantly expressed at the cell surface of diverse cell types and has been implicated in many biological functions involving cell adhesion, cell migration, cell proliferation, and metastasis (Naot *et al.*, 1997; Ponta *et al.*, 1998; Siegelman *et al.*, 1999). During migration, CD44 redistributes at the plasma membrane in a process that parallels the establishment of cell polarity in neutrophils (our unpublished observations) and fibroblasts (Jacobson *et al.*, 1984), making this molecule a reliable marker of cell polarity. CD44 has been shown to associate with DRMs in different cell types (Neame *et al.*, 1995; Ilangumaran *et al.*, 1998; Oliferenko *et al.*, 1999), and in epithelial cells it interacts simultaneously with DRMs and the actin cytoskeleton in basolateral membranes (Oliferenko *et al.*, 1999). These findings suggest that CD44 may play a role in organizing DRM distribution.

To investigate this possibility, we have used human neutrophils as a model system because they undergo rapid polarization in response to stimuli. In the present study, we investigate the kinetics of formation of DRMs during the establishment of polarity. To this end, we selected a set of membrane proteins and fluorescent lipid analogs on the basis of their predicted propensities to partition into DRMs (the GPI-anchored FcγRIII receptor CD16, CD44, and $DiIC_{16}$) or to be excluded from them (the transmembrane phosphatase CD45, and *FAST*-DiI), and we used these to probe the organization of the plasma membrane at various stages of polarity development. We also looked at the transmembrane glycoprotein CD43, a regulator of cell adherence, because like CD44, it is a marker of cell polarity (Seveau *et al.*, 1997, 2000); however, unlike CD44, CD43 has not previously been shown to associate with DRMs.

MATERIALS AND METHODS

Reagents and Antibodies

N-Formyl-L-methionyl-L-leucyl-L-phenylalanine (fMLF) and methyl-β-cyclodextrin (MβCD) were purchased from Sigma (St. Louis, MO). Human fibronectin was from Collaborative Biomedical Products (Becton Dickinson, Bedford, MA). Triton X-100 (TX-100) was purchased from Pierce (Rockford, IL). ECL Western blotting detection reagents were from Amersham Pharmacia Biotech (Buckinghamshire, UK). The protease inhibitor mixture (800 μg/ml benzamidine HCl, 500 μg/ml phenanthroline, 500 μg/ml aprotinin, 500 μg/ml leupeptin, 50 mM PMSF, 500 μg/ml pepstatin A) was from PharMingen (San Diego, CA). ML-7 was purchased from Alexis Corporation (San Diego, CA). The mouse mAbs anti-human CD43 (clone L60), CD16 (clone 3G8), CD45 (clone BRA-55), HLA-A, -B, -C (clone W6/32), and CD44 (clone J-173) were purchased from Becton Dickinson, PharMingen, Sigma, Harlan Sera-Lab (Leicestershire, United Kingdom), and Immunotech (Marseilles, France), respectively. Alternatively, anti-human CD44 mAb was purified from the Hermes-3 hybridoma (American Type Culture Collection, Manassas, VA), and it was determined that it gave the same labelling pattern by Western blotting and immunofluorescence as the J-173 clone (our unpublished data). Peroxidase-conjugated affinity-purified donkey anti-mouse IgG (H+L) antibodies were from Jackson Immunoresearch (West Grove, PA). Alexa Fluor 488-conjugated goat anti-mouse IgG (H+L) antibodies, Alexa Fluor 568 phalloidin, $DiIC_{16}$, *FAST*-DiI, and latrunculin A were from Molecular Probes (Eugene, OR).

Neutrophil Isolation

Neutrophils were prepared at room temperature from heparin-anticoagulated blood donated by healthy adult volunteers. Neutrophils were isolated by a one-step density gradient centrifugation on Polymorphprep (Nycomed, Oslo, Norway), according to the manufacturer's instructions. Residual erythrocytes were lysed in H_2O for 30 s, and the osmolarity of the medium was then equilibrated by addition of a 5× PBS solution. Cells were washed two times and resuspended in incubation medium M2 (150 mM NaCl, 5 mM KCl, 1 mM $MgCl_2$, 1 mM $CaCl_2$, 20 mM HEPES, pH 7.4).

Induction of Neutrophil Migration

As described previously (Marks *et al.*, 1991), neutrophils were allowed to settle at 37°C for 3–5 min (as indicated) on coverslip-bottom dishes coated with human fibronectin. Cells were then stimulated to migrate at 37°C by the addition of fMLF (10 nM in the incubation medium). After stimulation, the cells were immediately fixed (6.6% paraformaldehyde [PFA] in PBS), or extracted with 0.5% TX-100, and then fixed, or lysed in TX-100 (0.5%) for the density gradient centrifugation experiments, as mentioned in RESULTS.

Inhibition of Actin–Myosin Contraction

Neutrophils were allowed to settle at 37°C for 5 min on fibronectin-coated coverslips and then were incubated for an additional 5 min in the presence of 10 μM of the myosin light chain kinase inhibitor ML-7 (Eddy *et al.*, 2000). Cells were then stimulated by 10 nM fMLF in the presence of ML-7 for the indicated times.

TX-100 Extractions

After cell activation at 37°C, dishes were transferred to ice, and the cells were washed once with ice-cold cytoskeleton stabilization buffer (CSB: 138 mM KCl, 3 mM $MgCl_2$, 2 mM EGTA, 0.32 M sucrose, 10 mM MES, pH 6.1). The cells were then extracted on ice for the indicated time in CSB containing 0.5% TX-100 and protease inhibitor mixture (1:50). Where indicated, Alexa Fluor 568-phalloidin (1 U/ml) was added to the CSB extraction buffer. Cells were washed once with ice-cold CSB and then fixed (6.6% PFA in CSB) for 10 min on ice. In some experiments, cells were TX-100 extracted at room temperature with CSB containing 0.2% TX-100 for 5 min, then washed and fixed (6.6% PFA in CBS) at room temperature.

To assess the relative amount of CD44 associated with DRMs or with the cytoskeleton, suspended neutrophils (2×10^6/ml) were incubated in M2 for 5 min at 37°C, and then latrunculin A (1 μM) or MβCD (10 mM) was added in the medium for an additional 10 min. Cells were incubated with or without fMLF (10 nM) for 5 min (in the presence of latrunculin A or MβCD). Cells were then centrifuged, and the pellet was lysed in 0.5% TX-100 for 30 min. Cells lysates were centrifuged at 14,000 × *g* for 10 min, and the pellets (insoluble fractions) and supernatants (soluble fractions) were separated and analyzed by Western blotting for CD44. Western blots were ana-

lyzed by chemiluminescence, and the relative intensity of each band was determined with the use of the public software NIH Image 1.62 (http://www.tsc.udel.edu/macsoftdist/image.html).

Cellular Labeling

After fixation, cells were washed twice with 0.1 M glycine in PBS and then incubated in blocking solution (PBS, 10% fetal bovine serum) at room temperature for 30 min. Cells were incubated with mAbs (diluted in blocking solution) for 30 min at room temperature at the following concentrations: CD43 (25 μg/ml), CD44 (25 μg/ml), CD45 (25 μg/ml), CD16 (25 μg/ml), HLA-I (10 μg/ml). After washing with PBS, cells were incubated for an additional 30 min with Alexa Fluor 488-conjugated goat anti-mouse secondary antibody (1:600) in blocking solution and then washed and analyzed by confocal microscopy. F-actin labeling was performed either after fixation or during TX-100 extraction by addition of Alexa Fluor 568-conjugated phalloidin. In some experiments, neutrophils were prelabeled on ice with $DiIC_{16}$ (10 μM) for 20 s and then washed. For double-label experiments with $DiIC_{16}$ and antibodies, the cells were labeled for a shorter period of time (5 min instead of 30 min) with 5× concentrated antibody solutions to preserve DiC_{16} labeling.

Wide-field Microscopy and Fluorescence Quantification after TX-100 Extraction

Neutrophils adherent to fibronectin were activated by fMLF for 5 min at 37°C. Cells were extracted with either cold or room temperature TX-100 and then fixed and immunolabeled for CD44 with Alexa Fluor 488-conjugated antibodies. Fluorescence images were acquired on a Leica DMIRB fluorescence microscope (Leica Microsystems, Wetzler, Germany), equipped with a cooled charge-coupled device camera (Micromax 512BFT, Princeton Instruments, Princeton, NJ) driven by Metamorph Imaging System software (Universal Imaging, Downingtown, PA). Images were acquired with the use of a 63× oil immersion objective (1.32 NA). For quantification of fluorescence, all images were acquired under the same conditions (acquisition time and microscope settings). Images were background corrected, and a mask was applied to consider only the fluorescence associated with entire cells within the field. Fluorescence intensity per cell was calculated by the ratio of the total fluorescence intensity per field over the cell number within the field.

Confocal Microscopy

Confocal microscopy was performed with the use of an Axiovert 100 M microscope equipped with an LSM 510 laser scanning unit and a 63× 1.4 NA Plan Apochromat objective (Carl Zeiss, Inc., Jena, Germany). Alexa Fluor 488 was excited with the 488 nm line from an argon laser, and the emission was collected with a 505–530 nm bandpass filter. Alexa Fluor 568 was excited with the 546 nm line from a helium/neon laser and was collected with a long-pass filter. To avoid cross-talk in double-label experiments, the two channels were scanned alternatively, with only one laser and one detector on at any time. No cross-talk was detected between different channels.

Equilibrium Density Gradient Centrifugation

Neutrophils (5×10^6 cells) were lysed in 250 μl TKM buffer (50 mM Tris-HCl, pH 7.4, 25 mM KCl, 5 mM $MgCl_2$, and 1 mM EGTA) containing TX-100 (0.5%) and protease inhibitor mixture (1:50) for 30 min on ice according to Ilangumaran *et al.* (1998). The cell lysate was mixed with an equal volume of 80% sucrose containing 0.5% TX-100. Tubes were filled successively with 1 ml of 80% sucrose in TKM, 500 μl of 40% sucrose containing the cell lysate, 6 ml of 36% sucrose, and 3.5 ml of 5% sucrose. The gradients were centrifuged in a Beckman ultracentrifuge (rotor SW41) at 4°C for 18 h at 38,000 rpm. Fractions (1 ml) were collected from top to bottom, and proteins were precipitated with trichloroacetic acid. Samples corresponding to each fraction were analyzed by Western blotting for CD44, CD43, and CD45.

RESULTS

DRMs Are Located toward the Rear of Polarized Neutrophils

Neutrophils were plated onto fibronectin-coated dishes, stimulated to polarize and migrate with a bath application of fMLF, and then fixed and labeled for various membrane proteins. As shown in Figure 1A, the GPI-anchored CD16 and HLA appeared relatively evenly distributed across the surface of polarized neutrophils, in contrast to CD44 and CD43, which were concentrated at the uropod (Alonso-Lebrero *et al.*, 2000; Seveau *et al.*, 2000), and to CD45, which appeared to be accumulated toward the leading edge. The apparent enrichment of CD45 molecules toward the front of cells (Figure 1A) could be a consequence of folded membrane in ruffles. However, electron microscopy studies have shown that the number of CD45 molecules per unit of membrane area is indeed enhanced at that pole (Haston and Maggs, 1990). When polarized cells were first extracted with cold TX-100 (0.5%) for 30 min and then fixed and labeled for the various membrane proteins (Figure 1B), we observed an asymmetrical sensitivity of the proteins to extraction. All proteins studied were extracted at the leading edge, whereas a subset was retained toward the rear of the cells. HLA and CD45, which have been shown to be excluded from DRMs in lymphocytes (Rodgers and Rose, 1996), were completely and uniformly extracted from the plasma membrane. In contrast, CD43, CD44, and CD16 were partially resistant to extraction by cold TX-100 in the cell bodies and the uropods (Figure 1B). Although CD43 and CD44 were already enriched at the uropod before cell extraction, the comparison of CD16 distribution in Figure 1, A and B, shows that CD16 was preferentially extracted from the front of the cells. This suggests that CD16 in the front is in a different membrane environment from CD16 at the rear of the cells. Different concentrations of TX-100 (0.1–1%) in the extraction buffer did not affect the pattern of membrane protein extraction (our unpublished observations). Also, the effects on $DiIC_{16}$ extraction were the same at 0.5 or 1% TX-100 (our unpublished observations).

To determine whether the differential extractability of proteins between rear and front corresponded to a difference in the lipid environment, we labeled the cells with the fluorescent lipid analogs $DiIC_{16}$ and *FAST*-DiI. $DiIC_{16}$ has been used as a marker of DRM-like membranes in several studies (Thomas *et al.*, 1994; Pierini *et al.*, 1996) because it has the ability to partition into DRMs (although it also diffuses into more fluid domains) (Spink *et al.*, 1990), whereas *FAST*-DiI, with its unsaturated acyl chains, is relatively excluded from DRMs (Pierini *et al.*, 1996). As shown in Figure 2A, $DiIC_{16}$ (panels a′, a″) and *FAST*-DiI (panels b′, b″) appear to be distributed nearly homogeneously in polarized cells before detergent extraction. After cold TX-100 extraction, $DiIC_{16}$ is preferentially extracted from the leading lamella, but it is retained in the cell body and uropod (panels c′, c″). In contrast, *FAST*-DiI was completely and uniformly extracted from the plasma membrane (panels d′, d″). These results are in accordance with our results for membrane proteins, namely that the

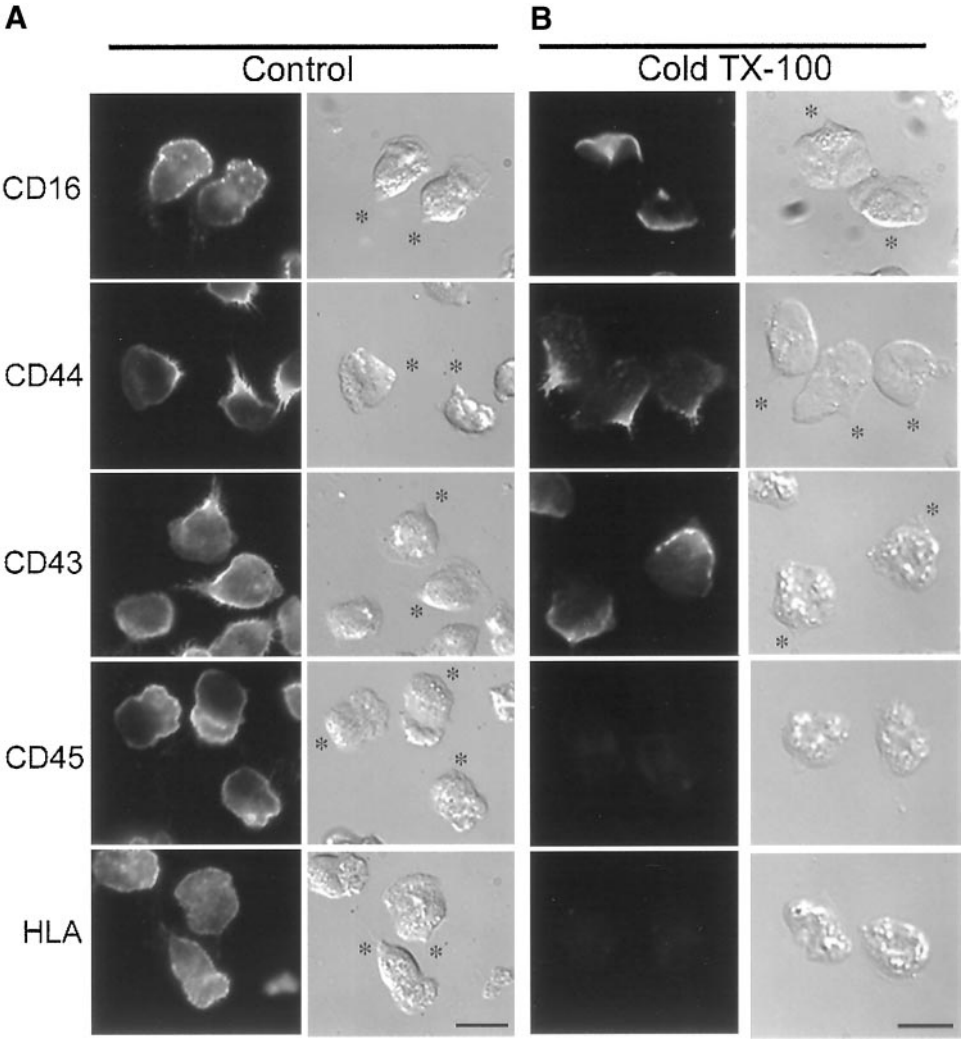

Figure 1. Extraction with cold Triton X-100 reveals DRM organization in polarized neutrophils. Neutrophils were activated at 37°C by fMLF (10 nM). After 5 min of stimulation, cells were fixed (A) or extracted with cold TX-100 (0.5% for 30 min) and then fixed (B). Membrane proteins were labeled as described in MATERIALS AND METHODS. Cells were analyzed by DIC and fluorescence wide-field microscopy. Asterisks indicate the position of the uropods. Bar, 10 μm.

plasma membrane comprising the rear pole of neutrophils is resistant to detergent extraction. It appears that the membrane of lamellipodia is completely extracted, because we could not find any membrane marker still present after cold TX-100 extraction. By DIC microscopy, lamellipodia are still visible after extraction (Figure 2), most likely because of the F-actin network that is retained at the leading edge in the extracted cells. To assess whether the rear pool of insoluble membrane proteins and $DiIC_{16}$ resided in a similar region of the plasma membrane, we performed colabeling experiments with $DiIC_{16}$ and CD43 or CD44 (Figure 2B). Neutrophils prelabeled with $DiIC_{16}$ were activated to migrate, then extracted with cold TX-100 and subsequently fixed and labeled for membrane proteins. To preserve $DiIC_{16}$ labeling, cells were immunostained using a fast protocol as described in MATERIALS AND METHODS, then immediately analyzed by confocal microscopy. As shown in Figure 2B, the insoluble lipids ($DiIC_{16}$) and proteins (CD43, CD44) colocalized within a region toward the rear of the cells.

The Rear Pool of DRMs Is Associated with the Cytoskeleton via CD44 and CD43

Insolubility of membrane proteins in cold detergents can be a consequence of an interaction of the proteins with either DRMs or the underlying cytoskeleton. To distinguish between these two possibilities, we performed TX-100 extraction at room temperature, which preserves cytoskeleton interactions but solubilizes DRMs. As shown in Figure 3A, F-actin labeled with Alexa Fluor 568-phalloidin was resistant to room temperature extraction with TX-100. In contrast, the GPI-linked CD16 was completely and uniformly extracted by TX-100 at room temperature, indicating that the portion of insoluble CD16 molecules observed after cold TX-100 extraction (Figure 1B) was indeed insoluble because of its association with DRMs. On the other hand, CD43 and CD44 molecules were still retained at the rear of cells after room temperature extraction, suggesting that their retention after cold extraction (Figures 1B and 2B) was due at least in part to an association with the cytoskeleton. This result is in agreement with previous data showing that CD43 and CD44

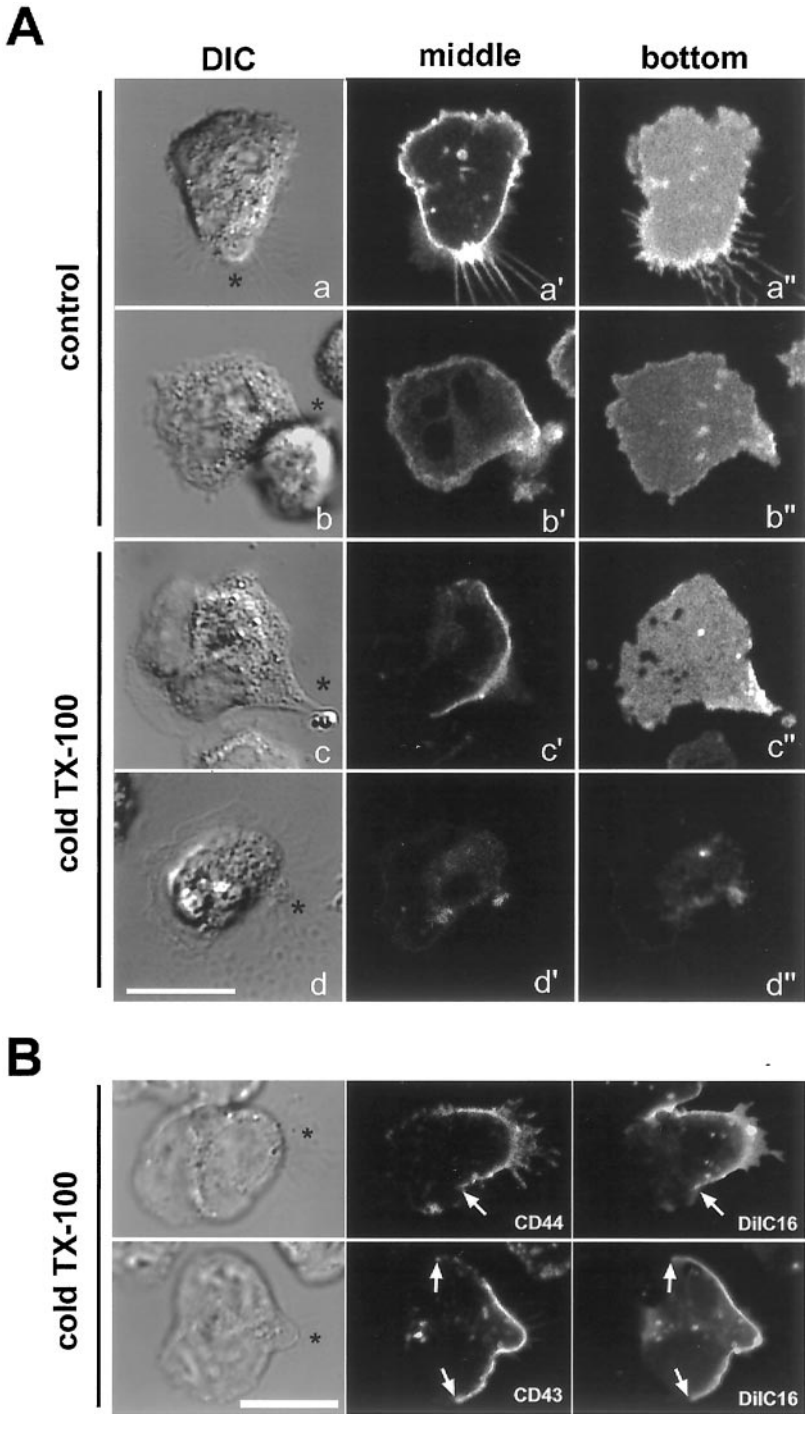

Figure 2. Detergent-resistant lipids and proteins localize to the same region of extracted neutrophils. (A) Neutrophils were prelabeled on ice with either $DiIC_{16}$ or *FAST*-DiI, then plated onto fibronectin-coated coverslips and stimulated with fMLF (10 nM). After 3 min of activation, cells were either imaged directly (a and b) or extracted with cold TX-100 (0.5% for 15 min) and then imaged (c and d). Images of cells labeled with $DiIC_{16}$ (a and c) or *FAST*-DiI (b and d) were acquired by confocal microscopy. DIC images (a–d) and confocal fluorescence images of middle planes (a′–d′) or of the bottom adherent membranes (a″–d″) are presented. (B) Cells were prelabeled on ice with $DiIC_{16}$, then plated onto fibronectin and stimulated with fMLF. After 3 min of activation, cells were extracted with cold TX-100 (0.5% for 15 min) and then fixed and labeled for CD44 or CD43. Cells were immediately analyzed by confocal microscopy. DIC and fluorescence images of representative single planes are presented. Asterisks (*) indicate the position of the uropods. Arrows delineate the borders between areas of the membrane that retain $DiIC_{16}$ and extracted areas. Bar, 10 μm.

molecules associate with the F-actin cytoskeleton via the ezrin/radixin/moesin (ERM) family members (Serrador *et al.*, 1998; Yonemura *et al.*, 1998; Seveau *et al.*, 2000). Quantification of the fluorescence retained at the cell surface after extraction showed that an additional 40% of CD44 molecules could be extracted at room temperature compared with extraction at 4°C (Figure 3B). This indicates that the association of CD44 molecules with the cytoskeleton does not completely account for their insolubility to cold TX-100. Similar results were obtained for CD43 (our unpublished data).

We hypothesized that CD43 and CD44 were interacting simultaneously with DRMs and the F-actin cytoskeleton, thereby connecting DRMs to the cytoskeleton. To test this

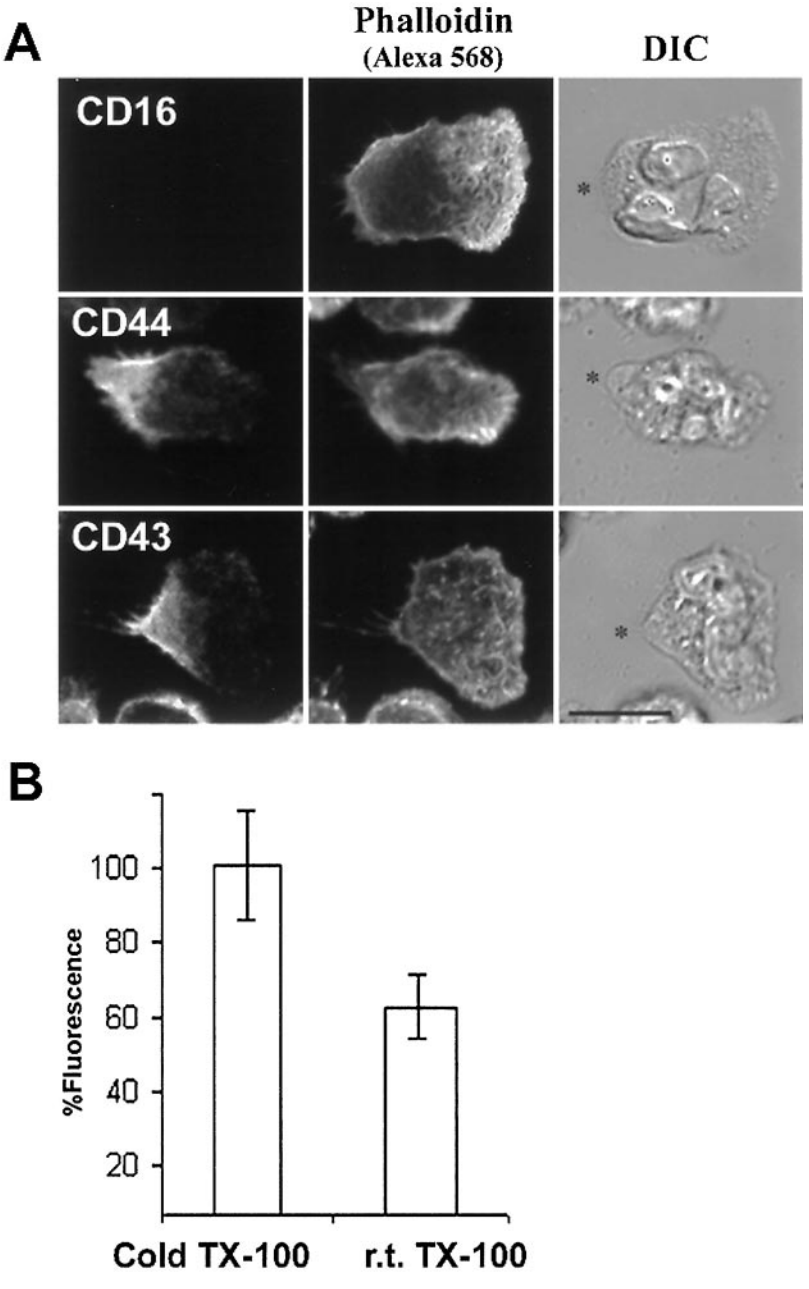

Figure 3. Detergent-resistance of CD43 and CD44, but not of CD16, is due in part to cytoskeletal association. (A) Neutrophils were activated on fibronectin at 37°C by fMLF (10 nM) for 5 min and then extracted with TX-100 (0.2% for 5 min in the presence of Alexa Fluor 568-phalloidin) at room temperature and fixed. Cells were labeled for CD44 or CD43 with Alexa Fluor 488-conjugated antibodies and analyzed by confocal microscopy. For CD16, cells were prelabeled with primary fluorescent antibodies before the experiment. DIC and projections of fluorescent confocal planes are presented. Asterisks (*) indicate the positions of the uropods. Bar, 10 μm. (B) After 5 min of migration, neutrophils were extracted with either cold or room temperature detergent, fixed, and labeled for CD44 with fluorescent antibodies. Fluorescence images were acquired by widefield microscopy, and the intensity of CD44 fluorescence per cell was determined for each condition, then normalized to the values obtained for extraction in the cold to allow comparison from different days' experiments. Results represent the average of three independent experiments.

hypothesis, we performed lipid floatation experiments. After TX-100 extraction, cell lysates were subjected to ultracentrifugation on sucrose gradients, in which proteins that are associated with DRMs float to low density, whereas soluble proteins or proteins associated with the cytoskeleton distribute to higher densities (Brown and Rose, 1992). After extraction with cold TX-100, cell lysates were adjusted to 40% sucrose and subjected to centrifugation on a sucrose gradient (5–80% sucrose). As presented in Figure 4A, we found CD44 and CD43 in both low-density (20% sucrose, fractions 4–6) and high-density fractions (40–80% sucrose, fractions 9–11). The presence of the molecules in the low-density fractions shows that a portion of CD44 and CD43 molecules associate with DRMs. The non-DRM protein, CD45, was not enriched in the low-density fractions. To further confirm this result, DRMs were disrupted by treating whole cells with the cholesterol chelator, MβCD, before extraction and ultracentrifugation. As shown in Figure 4B, after disruption of DRMs by MβCD, CD44 and CD43 were no longer recovered in the low-density fractions.

To assess whether the pool of CD44 and CD43 molecules engaged in DRMs was simultaneously associated with the cytoskeleton, we depolymerized F-actin with latrunculin A and found that the amount of CD44 and CD43 in the low-

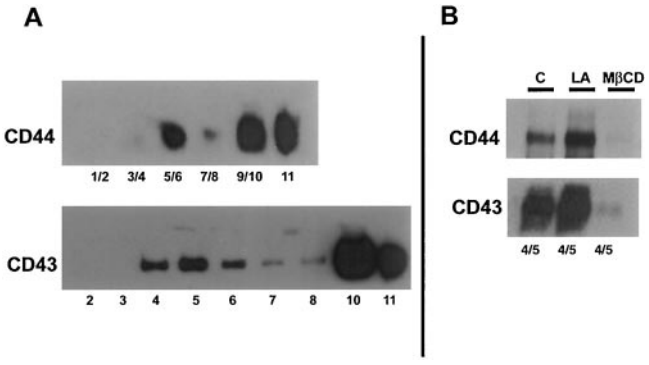

Figure 4. CD43 and CD44 are recovered in the DRM fractions of density gradients, and their association with these fractions is cholesterol and actin dependent. (A) Neutrophils were activated by fMLF on fibronectin-coated culture dishes for 5 min at 37°C and then extracted with cold TX-100 (0.5%) for 30 min. Dishes were scraped with a cell scraper, and lysates were subjected to centrifugation on a sucrose gradient (5–80%). Fractions were collected from top to bottom and analyzed by Western blotting with antibodies to CD44 or CD43. The low-density fractions correspond to fractions 4–6. (B) Suspended cells were preincubated in the presence of latrunculin A (LA) (1 μM) or MβCD (10 mM) for 10 min at 37°C; cells were then stimulated for 5 min with fMLF (10 nM). Cells were lysed and then subjected to ultracentrifugation as for A. The low-density fractions (4/5) were pooled and analyzed by Western blotting for CD44 and CD43.

density fractions was increased (Figure 4B). This suggests that when the F-actin cytoskeleton is intact, a portion of molecules associated with DRMs could not float to low density because of their cytoskeletal anchorage. Similar results have been observed for CD44 in epithelial cells (Oliferenko *et al.*, 1999).

We analyzed the relative amount of CD44 present within DRMs and associated with F-actin. To do so, we performed TX-100 extraction of resting and stimulated neutrophils under conditions that either preserved or disrupted the F-actin network or the DRMs. Cold TX-100 extraction preserves both the cytoskeleton and DRMs, whereas room temperature extraction solubilizes DRMs yet preserves the F-actin. Preincubation with latrunculin A disrupts the F-actin, and MβCD causes the disruption of DRMs. Resting and activated cells were incubated at 37°C with or without latrunculin A or MβCD and were then TX-100 extracted either at 4°C or at room temperature. After TX-100 extraction, the soluble and insoluble fractions were analyzed by Western blotting for CD44. As shown in Table 1, if both the cytoskeleton and the DRMs were preserved, a total of 55% of CD44 molecules were TX-100 insoluble. After F-actin depolymerization, 55% of CD44 molecules were still insoluble in cold TX-100. After lipid domain disruption, ~35% of CD44 molecules were TX-100 insoluble. Similar results were found for both resting and stimulated neutrophils.

Table 1. Neutrophils (2×10^6/ml) were treated with or without LA (1 μM) or MβCD (10 mM) in M2 at 37°C for 10 min

Temperature of extraction	4°C	25°C	4°C	4°C
Cell treatment			Latrunculin A (1 μM)	MβCD (10 mM)
Resting cells Insoluble CD44 (% ± STD)	56 ± 5	29 ± 13	55 ± 13	30 ± 30
Activated cells Insoluble CD44 (% ± STD)	53.5 ± 0.7	40 ± 0.7	60 ± 14	43 ± 10

Cells were incubated for an additional period of 10 min with (Activated cells) or without (Resting cells) fMLF (10 nM). The cells were then extracted in 0.5% TX-100 buffer at 4 or 25°C. After centrifugation, soluble and insoluble fractions were separated and electrophoresed under nonreducing conditions. CD44 molecules were detected by ECL-based Western blot, and the films were scanned and quantified (integrated density of each band) using NIH software version 1.62.

DRMs Become Asymmetrically Redistributed during the Establishment of Cell Polarity

We investigated whether DRMs were present at the plasma membrane before chemotactic stimulation, and we followed their distribution during the establishment of cell polarity. Neutrophils stimulated by fMLF undergo a succession of morphological changes as shown by the series of images in Figure 5. During the first 15 s of stimulation at 37°C, nonpolarized cells exhibited extensive ruffling (Figure 5, B and F). After 30 s, cells started to spread and send out multiple lamellipodia with no directionality (Figure 5, C and G). After 60 s, vectorially polarized cells presented a single lamellipodium and started to migrate (Figure 5, D and H). To follow DRM distribution in these cells, we examined the distribution of CD44 with or without extraction by cold TX-100. After 0, 15, 30, and 60 s of stimulation by fMLF, cells were fixed and immunostained for CD44 (Figure 5, A, A′, B, B′, C, C′, and D, D′). Before stimulation and up until 15 s after stimulation, CD44 molecules were uniformly distributed (Figure 5, A′ and B′). After 30 s, the multiple small lamellipodia appear to have a lower density of CD44 labeling (Figure 5C′) compared with plasma membrane just outside these extensions. After 60 s, CD44 molecules were clearly depleted from the leading lamella and concentrated at the rear of polarized cells (Figure 5D′).

To confirm that CD44 localization correlated with DRM localization, we extracted cells with cold TX-100 before fixation and CD44 labeling (Figure 5, E, E′, F, F′, G, G′, and H, H′). Before the addition of fMLF (0 s), DRMs were uniformly distributed at the plasma membrane, as indicated by a relatively solid ring of CD44 fluorescence (Figure 5E′). After 15 s of stimulation, DRMs were located over almost the entire cell surface in patches (Figure 5F′). After 30 s, the plasma membrane bordering the lamellipodial membranes was resistant to detergent extraction (Figure G′), similar to the rear of fully polarized cells (H′), whereas membrane overlying lamellipodia (G′) and leading lamellae (H′) was devoid of DRMs. The comparison of DRM distribution at 0, 15, 30, and 60 s of stimulation indicates that during the establishment of cell polarity, DRMs were redistributed

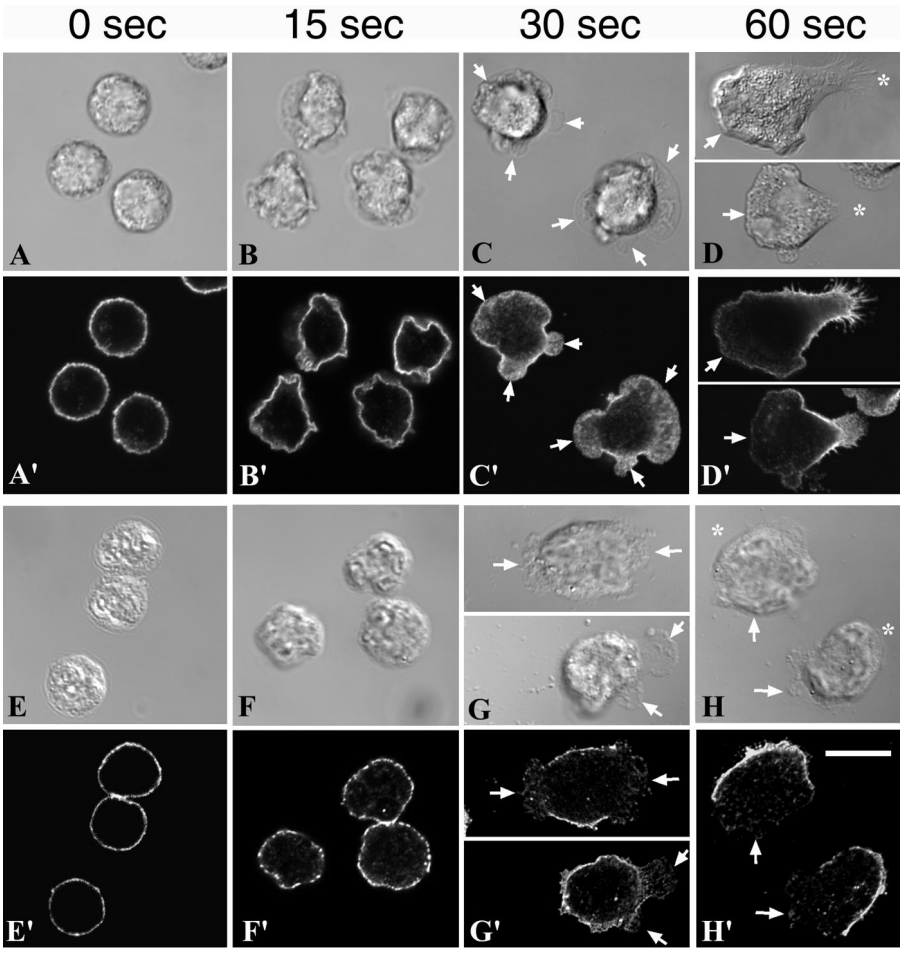

Figure 5. DRMs coalesce to the rear membranes during fMLF stimulation. Neutrophils were plated onto fibronectin-coated dishes, activated by fMLF (10 nM) for 0, 15, 30, and 60 s at 37°C, and then directly fixed and labeled for CD44 (A′–D′). Alternatively, cells were plated and stimulated as above, extracted with cold TX-100, and then fixed and labeled for CD44 (E′–H′). Arrows indicate ruffling areas of the plasma membrane. Bar, 10 μm.

from an initially uniform ring to an asymmetrical cap, with DRMs comprising the back end of polarized cells. Together, these data suggested that CD44-containing DRMs coalesced toward the rear of polarizing cells.

DRM Coalescence, but Not Patching, Is Dependent on Actin–Myosin Contraction

Because CD44 and CD43 molecules provide a linkage between F-actin and DRMs, we hypothesized that the cytoskeleton, acting through these molecules, could be involved in the localization and stabilization of DRMs. We investigated whether actin–myosin contractions were required for coalescence of DRMs by pretreating the cells with the myosin light chain kinase inhibitor, ML-7, before the addition of fMLF. In cell migration assays, we previously demonstrated that preincubation of neutrophils with 10 μM ML-7, followed by fMLF stimulation in the presence of ML-7, blocked both cell motility and polarization (Eddy *et al.*, 2000). The K_i measured in vitro for inhibition of myosin light chain kinase by ML-7 (300 nM) is much lower than the K_i for protein kinase C (42 μM) or protein kinase A (21 μM) (Saitoh *et al.*, 1987). In cells, concentrations higher than the K_i are typically required, perhaps because of efflux of the drugs or binding to cytoplasmic proteins. We cannot rule out the possibility of some inhibition of other protein kinases at the concentrations of ML-7 that we have used, but in our previous study, similar effects on polarization were seen with the use of several myosin inhibitors, indicating that myosin inhibition is the cause for effects on polarization (Eddy *et al.*, 2000).

Interestingly, we found that the initial clustering of DRMs into small patches was not affected by ML-7 treatment, but the subsequent steps were inhibited (Figure 6). Small DRM patches remained at the plasma membrane even after a full minute of chemotactic stimulation, suggesting that the mechanism of initial DRM remodeling is different from later steps, because coalescence of DRM patches into larger aggregates evidently requires the actin–myosin cytoskeleton.

$DiIC_{16}$-containing Coalescence of DRMs Is Correlated with Cortical F-Actin Structure

Because DRM remodeling toward the rear pole was dependent on actin–myosin contractions, we investigated the organization of the actin cytoskeleton as related to DRM localization. Cells prelabeled with $DiIC_{16}$ were activated by fMLF for 0, 15, 30, and 60 s at 37°C. After extraction with cold TX-100 and fixation, cells were labeled for F-actin with the use of fluorescent phalloidin. Figure 7 shows that two types of F-actin structures were observed: cortical actin that

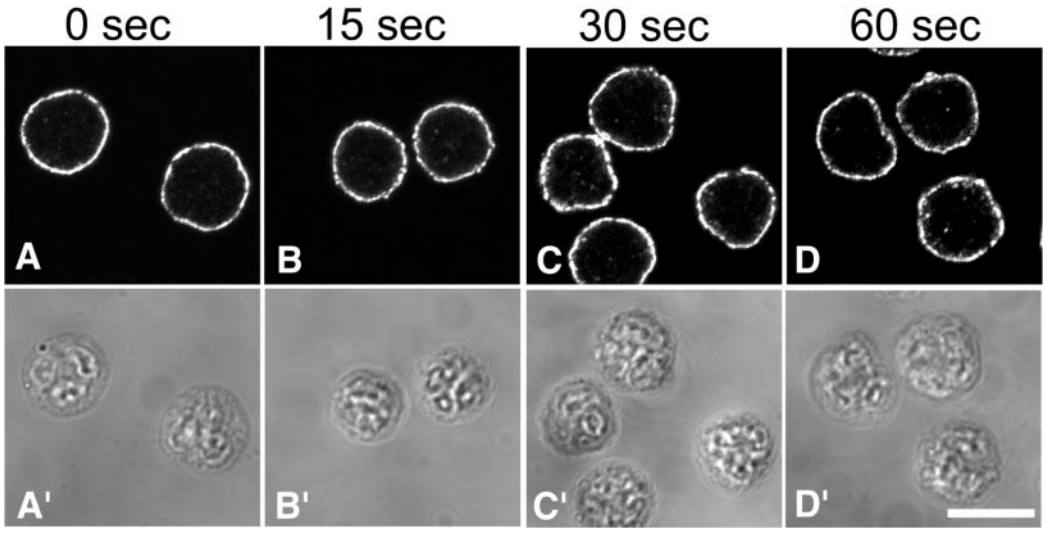

Figure 6. Stimulation-induced DRM coalescence is prevented by the inhibition of actin–myosin contraction. Neutrophils were plated onto fibronectin-coated coverslips for 5 min, incubated for an additional 5 min in the presence of ML-7 (10 μM), and then stimulated with a bath application of fMLF (10 nM) containing ML-7 (10 μM) for the indicated times. Cells were then extracted with cold TX-100, fixed, and labeled for CD44 to visualize DRMs.

appears in fluorescence micrographs as a smooth network and short F-actin bundles oriented perpendicular to the membrane in "finger-like" projections (Figure 7, arrows). Both types of F-actin structures were present at early stages of stimulation when multiple lamellipodia were pointed in all directions. At later stages, the network of cortical F-actin is localized to the cell body and uropod, whereas the finger-like network is restricted to the leading edge. Strikingly, after extraction with cold TX-100, which preserves F-actin structures as well as DRMs, we found that DRMs were always located just above the smooth cortical F-actin network and that the extracted membrane portions were always overlying the finger-like F-actin structures.

DISCUSSION

Neutrophil Plasma Membrane Is Composed Primarily of DRMs

Many studies have provided evidence that the plasma membrane is organized into lateral lipid domains of variable size (Varma and Mayor, 1998; Jacobson and Dietrich, 1999; Pralle *et al.*, 2000). The existence of domains of cholesterol-dependent phase-separated lipids has been demonstrated in artificial membrane models (Brown, 1998; Korlach *et al.*, 1999), and recent data support the formation of similar domains in biological membranes as well (Simons and Ikonen, 1997; Brown and London, 1998a,b, 2000). Formation of a liquid-ordered phase is thought to confer detergent resistance to the glycolipid-enriched DRMs (Ahmed *et al.*, 1997; Rietveld and Simons, 1998). Our approach to examine membrane domain organization in human neutrophils took advantage of the characteristic insolubility of some types of lipid domains in cold nonionic detergents and allowed us to demonstrate that a large proportion of the plasma membrane area of polarized neutrophils is resistant to extraction by cold nonionic detergents, as shown in Figures 1, 2, 5, and 7. This is in contrast to some models in which some types of DRMs are described as a minor component of the plasma membrane that exist as submicroscopic entities (~70–300 nm) dispersed within a mostly fluid membrane (Varma and Mayor, 1998; Jacobson and Dietrich, 1999). Previous studies have shown that much of the plasma membrane appears to be DRM-like because a large fraction of the surface area of many cells is resistant to extraction with cold TX-100 (Mayor and Maxfield, 1995; Hao M. *et al.*, in press). Our optical microscopy observations cannot detect the organization of lipid domains below the resolution threshold, and submicroscopic microdomains of varying properties may be intermixed in different regions of the cell before detergent extraction. These microdomains might coalesce into larger domains after detergent treatment.

DRM Organization in Polarized Neutrophils

The simplest interpretation of our findings, based on our detergent extraction experiments, might be that the plasma membrane of polarized neutrophils contains DRMs solely at the cell rear, whereas more fluid domains comprise the leading lamella. The fact that CD45, which has been shown to be excluded from DRMs in neutrophils (Figure 1) and T-cells (Rodgers and Rose, 1996), was concentrated toward the leading lamella is consistent with a more fluid organization of the membrane at the front of cells. This model is further supported by the observation that the DRM component CD44 (Figure 4) (Neame *et al.*, 1995) is concentrated toward the uropods of polarized cells both before and after cold detergent extraction. However, *FAST*-DiI, a lipid marker of fluid domains, was not enriched toward the leading edge, and the DRM markers $DiIC_{16}$ and the GPI-anchored CD16 were not biased toward the rear of cells before cold detergent extraction (Figures 1 and 2). Thus, it is clear that the differences in lipid organization and the distribution of lipid constituents are somewhat complex, and treatment with cold TX-100 reveals that the lipid properties differ at the front and rear of the cell. The differential detergent sensitivity of GPI-anchored proteins at the front and rear can be understood by comparison with studies in model membranes in which it was shown that the solubility of GPI-anchored proteins in cold TX-100 is dependent on the other

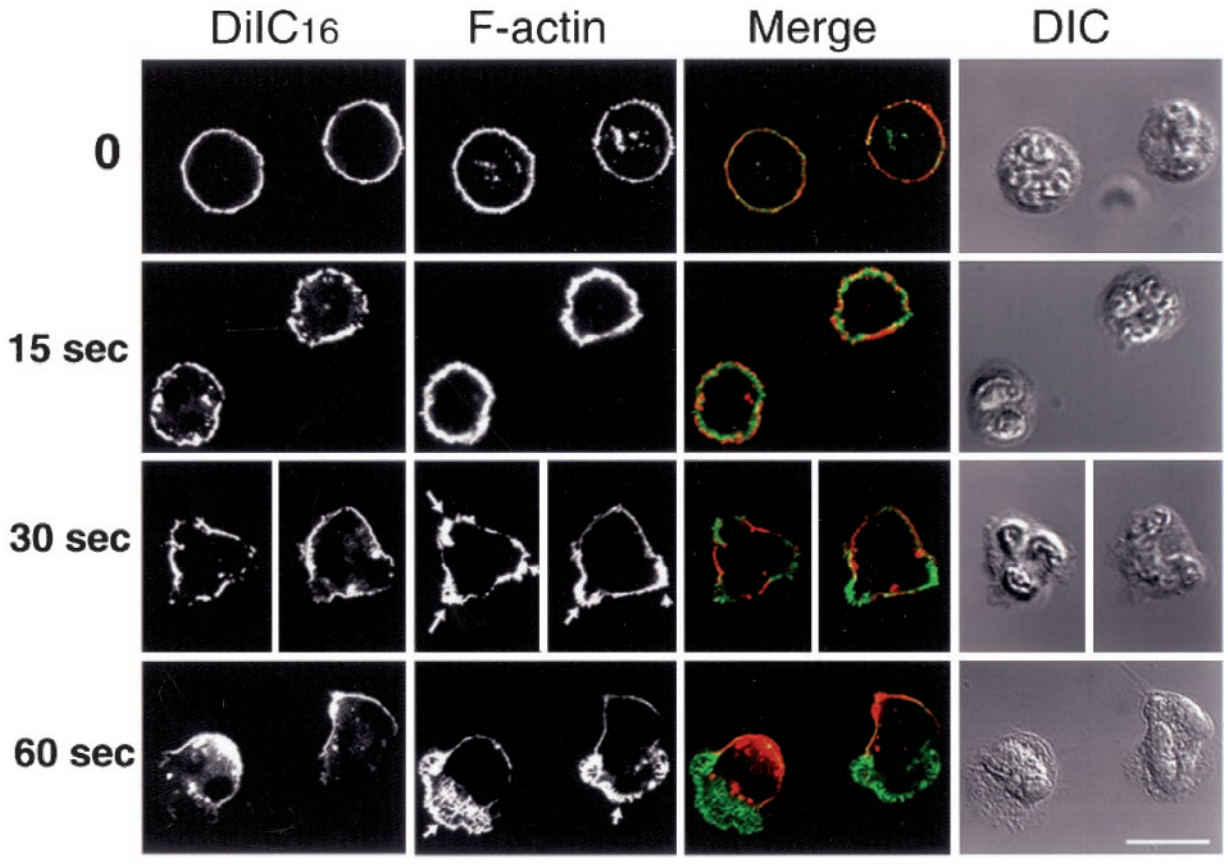

Figure 7. Stimulation-induced DRM coalescence correlates with cortical F-actin structure. Neutrophils were prelabeled on ice with $DiIC_{16}$, then plated onto fibronectin and activated by fMLF (10 nM) for 0, 30, and 60 s at 37°C. Cells were extracted with cold TX-100 (0.5%) for 30 min in the presence of Alexa Fluor-488-conjugated phalloidin, then fixed and immediately analyzed by confocal microscopy. Single confocal planes are presented. Bar, 10 μm.

lipid components of the membranes (Brown and Rose, 1992). In neutrophils, the distribution of GPI-anchored proteins, such as CD16 and uPAR receptors, has been shown to be dependent on their association with transmembrane proteins (Kindzelskii *et al.*, 1996), suggesting that multiple processes control GPI distribution. It appears that the differences in membrane properties at the front and rear of polarized neutrophils are sufficient to confer differences in detergent sensitivity, although they do not cause large differences in partitioning preferences for GPI anchors or the fluorescent lipid analogs that we used. It should be noted that the DRM organization that we find in polarized neutrophils differs from the interpretation given to studies in migrating melanoma cells (Manes *et al.*, 1999); however, the characterization of the lipid organization in the melanoma cells was based mainly on the effects of cholesterol depletion.

Mechanism of Establishing and Maintaining Asymmetrical DRM Distribution

We have shown that DRMs are uniformly distributed at the plasma membrane of unstimulated cells at the resolution of optical microscopy. After stimulation with chemotactic peptides, DRMs become asymmetrically distributed as the cells polarize (Figures 5 and 7). The redistribution of DRMs toward the uropod is reminiscent of the redistribution of the adhesion molecules CD43, CD44, ICAM, and PSGL-1 (Dore *et al.*, 1996; Sanchez-Madrid and del Pozo, 1999; Seveau *et al.*, 2000). These molecules are concentrated at the uropods of polarized leukocytes, and they are associated with ERM family members (Serrador *et al.*, 1998; Yonemura *et al.*, 1998; Seveau *et al.*, 2000), which are proposed to link the plasma membrane to the F-actin cytoskeleton (Pestonjamasp *et al.*, 1995). Moesin, the major ERM identified in neutrophils (our unpublished results) colocalized with CD43 during the various stages of neutrophil polarization (Seveau *et al.*, 2000). Two models have been proposed to account for the rearward redistribution of membrane structures during cell migration (Bretscher, 1996). The first model proposed that the rearward redistribution is the consequence of a retrograde lipid flow most probably caused by oriented recycling of membrane. In the second model, the rearward flow of F-actin would sweep back any surface structure to which it is connected. Direct evidence from photobleaching of plasma membrane labeled with lipid analogs refutes the existence of

retrograde lipid flow in migrating human neutrophils (Lee *et al*., 1990). Because involvement of the F-actin cytoskeleton in the rearward redistribution of membrane proteins seems most likely, we postulated that DRM redistribution could be mediated by CD43/CD44 linkage to the F-actin cytoskeleton with the force provided by the motor protein myosin II. When actin–myosin contractions were inhibited by the myosin light chain kinase inhibitor, ML-7, the formation of DRM patches was unaffected, but the coalescence of these patches into a cap at the uropod was inhibited (Figure 6). This suggests that the DRM patches are pulled rearward by myosin, requiring a linkage of the DRMs to the actin cytoskeleton. Confirming this hypothesis, we found that approximately half of the CD44 molecules were present within DRMs and connected to the F-actin network on the basis of detergent insolubility under various conditions (Table 1). Similarly, in epithelial cells, CD44 is concomitantly located within DRMs and associated with the actin cytoskeleton (Oliferenko *et al*., 1999). Although the transmembrane domain of CD44 is sufficient for its partitioning into DRMs (Perschl *et al*., 1995), the intracellular domain of CD44, which mediates association with the cytoskeleton, was necessary for the correct distribution of CD44-containing DRMs to the basolateral membrane (Neame and Isacke, 1993). Our findings, taken together with the work in epithelial cells, support a model in which cytoskeletal anchorage of domains by transmembrane molecules such as CD44 governs the position of DRMs at the rear of polarized cells.

DRMs as Polarity Organizing Centers

It has been shown that after stimulation by chemotactic peptides, some components of the signaling pathways controlling actin polymerization were asymmetrically targeted to the plasma membrane in the amoebae *Dictyostelium*, leukocytes, and fibroblasts (Parent *et al*., 1998; Parent and Devreotes, 1999; Jin *et al*., 2000; Servant *et al*., 2000; Pierini L.M. *et al*., 2000). Such asymmetrical targeting of signaling molecules could account for the successive establishment and maintenance of cell polarity; however, the mechanism controlling the spatial localization of signaling molecules during polarization and migration is still unresolved. It has been proposed that polarized recruitment and activation of signaling molecules could be achieved by a compartmentalized plasma membrane (Manes *et al*., 1999; Pierini L.M. *et al*., 2000). The results presented here provide several lines of support for this hypothesis. First, we show that the plasma membrane of fully polarized neutrophils is compartmentalized into domains that are segregated into each pole of the cell. These different domains are not detectable before cell stimulation, when the DRMs are uniformly distributed at the plasma membrane. Second, each stage in cell shape change leading to the establishment of polarity is characterized by a change in DRM organization, which culminates with an asymmetrical cap of DRMs at the rear of fully polarized cells. Third, there is a striking correlation between the localization of the DRMs and the underlying F-actin structure. After 30 s of stimulation, cells were not yet polarized, but nonoriented F-actin ruffles projected from the cells. After 60 s, polarized cells were characterized by a single lamellipodium at the leading edge. At both times, the membrane portion containing DRM structures was always located outside the lamellipodia, suggesting that F-actin structure and membrane organization are closely related to each other. These results are in agreement with our recent observation that Rac, a small GTPase important for actin polymerization in neutrophils (Roberts *et al*., 1999; Glogauer *et al*., 2000), is specifically recruited at the leading edge outside the DRMs (Pierini L.M. *et al*., 2000). In our model, DRMs that are linked to the cytoskeleton via CD43/CD44 distribute to the rear of polarized cells and may act to exclude some signaling molecules (such as CD45 or Rac) or recruit others (e.g., Src family tyrosine kinases). The DRMs that are identified would inhibit the formation of lamellipodia at the back of polarized cells and consequently constrain their formation in permissive non-DRM structures at the cell front.

ACKNOWLEDGMENTS

We thank Drs. Bob Vasquez, Sharron Lin, Daniel Wuestner, Mingming Hao, and Melanie Brazil for critical reading and helpful comments on the manuscript. We thank other members of the Maxfield laboratory for helpful discussions. This work was supported by National Institutes of Health (NIH) grant GM34770 (F.R.M.). S.M.S. was supported by a fellowship from the Association pour la Recherche contre le Cancer Association, Paris. L.M.P. was supported by NIH National Research Service Award grant GM19058 and the Atorvastatin Research Award from Pfizer/Parke Davis.

REFERENCES

Ahmed, S.N., Brown, D.A., and London, E. (1997). On the origin of sphingolipid/cholesterol-rich detergent-insoluble cell membranes: physiological concentration of cholesterol and sphingolipid induce formation of a detergent-insoluble, liquid-ordered lipid phase in model membranes. Biochemistry *36*, 10944–10953.

Alonso-Lebrero, J.L., Serrador, J.M., Dominguez-Jimenez, C., Barreiro, O., Luque, A., del Pozo, M.A., Snapp, K.S., Kansas, G., Schwartz-Albiez, R., Furthmayr, H., Lozano, F., and Sanchez-Madrid, F. (2000). Polarization and interaction of adhesion molecules P-selectin glycoprotein ligand 1 and intercellular adhesion molecule 3 with moesin and ezrin in myeloid cells. Blood *95*, 2413–2419.

Bretscher, M.S. (1996). Getting membrane flow and the cytoskeleton to cooperate in moving cells. Cell *87*, 601–606.

Brown, D.A., and London, E. (1998a). Functions of lipid rafts in biological membranes. Annu. Rev. Cell Dev. Biol. *14*, 111–136.

Brown, D.A., and London, E. (1998b). Structure and origin of ordered lipid domains in biological membranes. J. Membr. Biol. *164*, 103–114.

Brown, D.A., and London, E. (2000). Structure and function of sphingolipid- and cholesterol-rich membrane rafts. J. Biol. Chem. *275*, 17221–17224.

Brown, D.A., and Rose, J.K. (1992). Sorting of GPI-anchored proteins to glycolipid-enriched membrane subdomains during transport to the apical cell surface. Cell *68*, 533–544.

Brown, R.E. (1998). Sphingolipid organization in biomembranes: what physical studies of model membrane reveal. J. Cell Sci. *111*, 1–9.

Deans, J.P., Robbins, S.M., Polyak, M.J., and Savage, J.A. (1998). Rapid redistribution of CD20 to a low density detergent-insoluble membrane compartment. J. Biol. Chem. *273*, 344–348.

Dore, M., Burns, A.R., Hughes, B.J., Entman, M.L., and Smith., C.W. (1996). Chemoattractant-induced changes in surface expression and redistribution of a functional ligand for P-selectin on neutrophils. Blood *87*, 2029–2037.

Eddy, R.J., Pierini, L.M., Matsumura, F., and Maxfield, F.R. (2000). Ca2+-dependent myosin II activation is required for uropod retraction during neutrophil migration. J. Cell Sci. *113*, 1287–1298.

Field, K.A., Holowka, D., and Baird, B. (1997). Compartmentalized activation of the high affinity immunoglobulin E receptor within membrane domains. J. Biol. Chem. *272*, 4276–4280.

Glogauer, M., Hartwig, J., and Stossel, T. (2000). Two pathways through Cdc42 couple the N-formyl receptor to actin nucleation in permeabilized human neutrophils. J. Cell Biol. *150*, 785–796.

Haston, W.S., and Maggs, A.F. (1990). Evidence for membrane differentiation in polarised leukocytes: the distribution of surface antigens analyzed with Ig-gold labeling. J. Cell Sci. *95*, 471–479.

Hao, M., Mukherjee, S., and Maxfield, F.R. Cholesterol depletion induces large-scale domain segregation in living cell membranes. Proc. Natl. Acad. Sci. USA. (in press).

Holowka, D., Sheets, E.D., and Baird, B. (2000). Interactions between Fc(epsilon)RI and lipid raft components are regulated by the actin cytoskeleton. J. Cell Sci. *113*, 1009–1019.

Ilangumaran, S., Briol, A., and Hoessli, D.C. (1998). CD44 selectively associates with active Src family protein tyrosine kinases Lck and Fyn in glycosphingolipid-rich plasma membrane domains of human peripheral blood lymphocytes. Blood *91*, 3901–3908.

Jacobson, K., and Dietrich, C. (1999). Looking at lipid rafts? Trends Cell Biol. *9*, 87–89.

Jacobson, K., O'Dell, D., Holifield, B., Murphy, T.L., and August, J.T. (1984). Redistribution of a major cell surface glycoprotein during cell movement. J. Cell Biol. *99*, 1613–1623.

Jin, T., Zhang, N., Long, Y., Parent, C.A., and Devreotes, P.N. (2000). Localization of the G protein $\beta\gamma$ complex in living cells during chemotaxis. Science *287*, 1034–1036.

Keller, P., and Simons, K. (1998). Cholesterol is required for surface transport of influenza virus hemagglutinin. J. Cell Biol. *140*, 1357–1367.

Kindzelskii, A.L., Laska, Z.O., Todd, R.F., and Petty, H.R. (1996). Urokinase-type plasminogen activator receptor reversibly dissociates from complement receptor type 3 (a Mb 2/CD11b/CD18) during neutrophil polarization. J. Immunol. *156*, 297–309.

Korlach, J., Schwille, P., Webb, W.W., and Feigenson, G.W. (1999). Characterization of lipid bilayer phases by confocal microscopy and fluorescence correlation spectroscopy. Proc. Natl. Acad. Sci. USA *96*, 8461–8466.

Lauffenburger, D.A., and Horwitz, A.F. (1996). Cell migration: a physically integrated molecular process. Cell *84*, 359–369.

Lee, J., Gustafsson, M., Magnusson, K.E., and Jacobson, K. (1990). The direction of membrane lipid flow in locomoting polymorphonuclear leukocytes. Science *247*, 1229–1233.

Manes, S., Mira, E., Gomez-Mouton, C., Lacalle, R.A., Keller, P., Labrador, J.P., and Martinez, A.C. (1999). Membrane raft microdomains mediate front-rear polarity in migrating cells. EMBO J. *18*, 6211–6220.

Manes, S., Lacalle, R.A., Gomez-Mouton, C., Real, G., Mira, E., and Martinez, A.C. (2001). Membrane raft microdomains in chemokine receptor function. Semin. Immunol. *13*, 147–157.

Marks, P.W., Hendy, B., and Maxfield, F.R. (1991). Attachment to fibronectin or vitronectin makes human neutrophil migration sensitive to alterations in cytosolic free calcium concentration. J. Cell. Biol. *112*, 149–158.

Mayor, S., and Maxfield, F.R. (1995). Insolubility and redistribution of GPI-anchored proteins at the cell surface after detergent treatment. Mol. Biol. Cell *6*, 929–944.

Mitchison, T.J., and Cramer, L.P. (1996). Actin-based cell motility and cell locomotion. Cell *84*, 371–379.

Naot, D., Sionov, R.V., and Ish-Shalom, D. (1997). CD44: structure, function, and association with the malignant process. Adv. Cancer Res. *71*, 241–319.

Neame, S.J., and Isacke, C.M. (1993). The cytoplasmic tail of CD44 is required for basolateral localization in epithelial MDCK cells but does not mediate association with the detergent-insoluble cytoskeleton of fibroblasts. J. Cell Biol. *121*, 1299–1310.

Neame, S.J., Uff, C.R., Sheikh, H., Wheatley, S.C., and Isacke, C.M. (1995). CD44 exhibits a cell type dependent interaction with Triton X-100 insoluble, lipid rich, plasma membrane domains. J. Cell Sci. *108*, 3127–3135.

Oliferenko, S., Paiha, K., Harder, T., Gerke, V., Schwarzler, C., Schwarz, H., Beug, H., Gunthert, U., and Huber, L.A. (1999). Analysis of CD44-containing lipid rafts: recruitment of annexin II and stabilization by the actin cytoskeleton. J. Cell Biol. *146*, 843–854.

Parent, C.A., Blacklock, B.J., Froehlich, W.M., Murphy, D.B., and Devreotes, P.N. (1998). G protein signaling events are activated at the leading edge of chemotactic cells. Cell *95*:81–91.

Parent, C.A., and Devreotes, P.N. (1999). A cell's sense of direction. Science *284*, 765–770.

Perschl, A., Lesly, J., English, N., Hyman, R., and Trowbridge, I.S. (1995). Transmembrane domain of CD44 is required for its detergent insolubility in fibroblasts. J. Cell Sci. *108*, 1033–1041.

Pestonjamasp, K., Amieva, M.R., Strassel, C.P., Nauseef, W.M., Furthmayr, H., and Luna, E.J. (1995). Moesin, ezrin, and p205 are actin-binding proteins associated with neutrophil plasma membranes. Mol. Biol. Cell *6*, 247–259.

Pierini, L., Holowka, D., and Baird, B. (1996). Fc epsilon RI-mediated association of 6-micron beads with RBL-2H3 mast cells results in exclusion of signaling proteins from the forming phagosome and abrogation of normal downstream signaling. J. Cell Biol. *134*, 1427–1439.

Pierini, L.M., Furoles, M., Seveau, S., Casulo, C., and Maxfield, F.R. Membrane cholesterol is critical for asymmetric Rac targeting during human neutrophil migration. In: American Society for Cell Biology 40th annual meeting program; 2000 Dec. 9–13, San Francisco, CA. (Abstract 2921).

Ponta, H., Wainwright, D., and Herrlich, P. (1998). The CD44 protein family. Int. J. Biochem. Cell Biol. *30*, 299–305.

Pralle, A., Keller, P., Florin, E.L., Simons, K., and Horber, J.K. (2000). Sphingolipid-cholesterol rafts diffuse as small entities in the plasma membrane of mammalian cells. J. Cell Biol. *148*, 997–1008.

Rietveld, A., and Simons, K. (1998). The differential miscibility of lipids as the basis for the formation of functional membrane rafts. Biochem. Biophys. Acta *1376*, 467–479.

Roberts, A.W., Kim, C., Zhen, L., Lowe, J.B., Kapur, R., Petryniak, B., Spaetti, A., Pollock, J.D., Borneo, J.B., Bradford, G.B., Atkinson, S.J., Dinauer, M.C., and Williams, D.A. (1999). Deficiency of the hematopoietic cell-specific Rho family GTPase Rac2 is characterized by abnormalities in neutrophil function and host defense. Immunity *10*, 183–196.

Rodgers, W., and Rose, J.K. (1996). Exclusion of CD45 inhibits activity of p56lck associated with glycolipid-enriched membrane domains. J. Cell Biol. *135*, 1515–1523.

Sanchez-Madrid, F., and del Pozo, M.A. (1999). Leukocyte polarization in cell migration and immune interactions. EMBO J. *18*, 501–511.

Saitoh, M., Ishikawa, T., Matsushima, S., Naka, M., and Hidaka, H. (1987). Selective inhibition of catalytic activity of smooth muscle myosin light chain kinase. J. Biol. Chem. *262*, 7796–7801.

Serrador, J.M., Nieto, M., Alonso-Lebrero, J.L., del Pozo, M.A., Calvo, J., Furthmayr, H., Schwartz-Albiez, R., Lozano, F., Gonzalez-Amaro, R., Sanchez-Mateos, P., and Sanchez-Madrid, F. (1998). CD43 interacts with moesin and ezrin and regulates its redistribution to the uropods of T lymphocytes at the cell-cell contacts. Blood *91*, 4632–4644.

Servant, G., Weiner, O.D., Herzmark, P., Balla, T., Sedat, J.W., and Bourne, H.R. (2000). Polarization of chemoattractant receptor signaling during neutrophil chemotaxis. Science *287*, 1037–1040.

Seveau, S., Keller, H., Maxfield, F.R., Piller, F., and Halbwachs-Mecarelli, L. (2000). Neutrophil polarity and locomotion are associated with surface redistribution of leukosialin (CD43), an antiadhesive membrane molecule. Blood *95*, 2462–2470.

Seveau, S., Lopez, S., Lesavre, P., Guichard, J., Cramer, E.M., and Halbwachs-Mecarelli, L. (1997). Leukosialin (CD43, sialophorin) redistribution in uropods of polarized neutrophils is induced by CD43 cross-linking by antibodies, by colchicine or by chemotactic peptides. J. Cell Sci. *110*, 1465–1475.

Siegelman, M.H., DeGrendele, H.C., and Estess, P. (1999). Activation and interaction of CD44 and hyaluronan in immunological systems. J. Leuk. Biol. *66*, 315–321.

Simons, K., and Ikonen, E. (1997). Functional rafts in cell membranes. Nature *387*, 569–572.

Spink, C.H., Yeager, M.D., and Feigenson, G.W. (1990). Partitioning behavior of indocarbocyanines probes between coexisting gel and fluid phases in model membranes. Biochim. Biophys. Acta *1023*, 25–33.

Thomas, J.L., Holowka, D., Baird, B., and Webb, W.W. (1994). Large-scale co-aggregation of fluorescent lipid probes with cell surface proteins. J. Cell Biol. *125*, 795–802.

Varma, R., and Mayor, S. (1998). GPI-anchored proteins are organized in submicron domains at the cell surface. Nature *394*, 798–801.

Yonemura, S., Hirao, M., Doi, Y., Takahashi, N., Kondo, T., and Tsukita, S. (1998). Ezrin/radixin/moesin (ERM) proteins bind to a positively charged amino acid cluster in the juxta-membrane cytoplasmic domain of CD44, CD43, and ICAM-2. J. Cell Biol. *140*, 885–895.